KERNEL ESTIMATION FOR TIME-FREQUENCY DISTRIBUTIONS USING EPIGRAPH SET OF L1-NORM

Zeynel Deprem, A. Enis Çetin

Electrical and Electronics Engineering Department
Bilkent University, Ankara,Turkey
zdeprem@ee.bilkent.edu.tr, cetin@bilkent.edu.tr

ABSTRACT

In this article, a new kernel estimation method is introduced using the epigraph set of the l_1-norm. The new method produces a high-resolution and cross-term free estimates for Cohen's Class of Time-frequency (TF) distributions. The kernel estimation process starts with an initial rough TF distribution. This initial estimate is orthogonally projected onto the epigraph set of the l_1 norm in TF domain. Epigraph set of the l_1 norm produces a sparse time-frequency distribution. Sparsity in TF domain leads to cross-term free TF distributions. Experimental results are presented and the TF distributions obtained with the estimated kernel are compared to those obtained with an optimized kernel.

Index Terms— Time-frequency distributions, Cohen's Class, L1-norm, sparsity

1. INTRODUCTION

Signals with time-varying frequency content are encountered in many areas, such as AM/FM communication [1], radar [2], sonar applications, medicine, audio and speech. An important requirement for these types of signals is the identification of separate components forming the signal in time-frequency (TF) plane. High resolution TF distributions or representations are needed to extract TF components of a given signal.

Short Time Fourier Transform (STFT) [3] and Wigner-Ville (WV) distribution [4] are the classical tools that are being used for TF analysis. STFT is a linear and relatively easier transformation. But a good resolution requires a proper window selection and we can not obtain high resolution both for time and frequency axis at the same time. WV is a distribution which provides the high resolution. But, as a result of its quadratic definition, together with the actual signal components that we would like to identify, it also creates so called cross-components or cross-terms. For this purpose, members of Cohen's class [5] which is generalization of WV distribution are used. In these types of distributions, the aim is to design the kernel of Cohen's class distribution to have a high resolution TF distribution which does not include cross-terms.

In this article a signal dependent kernel estimation method, having only two steps, is proposed for a Cohen's class distribution. In the first step a distribution is obtained using an initial rough Gaussian kernel. In the second step this distribution is projected onto the epigraph set of l_1 norm and a signal dependent kernel is obtained. Resulting high resolution distribution do not contain cross-terms. Cohen's class distributions are reviewed in Section 2, kernel design method is introduced in Section 3. Experimental results are presented in Section 4.

2. COHEN'S CLASS DISTRIBUTIONS

The Wigner-Ville (WV) distribution for a signal $x(t)$ is given by,

$$W_x(t,f) = \int_{-\infty}^{+\infty} x(t+\tau/2)x^*(t-\tau/2)e^{-j2\pi f\tau}d\tau. \quad (1)$$

A generalization of the WV distribution is the Cohen's class distribution which is given by,

$$P_x(t,f) = \int_{-\infty}^{+\infty}\int_{-\infty}^{+\infty} A_x(\theta,\tau)\Phi(\theta,\tau)e^{-j2\pi\theta t-j2\pi f\tau}d\theta d\tau. \quad (2)$$

where $A_x(\theta,\tau)$ is the ambiguity function (AF) and has a 2D Fourier transform relation with WV distribution. Ambiguity function is the basic tool in many target detection applications and is expressed as,

$$A_x(\theta,\tau) = \int_{-\infty}^{+\infty} x(t+\tau/2)x^*(t-\tau/2)e^{j2\pi\theta t}dt. \quad (3)$$

In Equation (2) $\Phi(\theta,\tau)$ represents the kernel of the Cohen's class distribution and $\Phi(\theta,\tau) = 1$ corresponds to the WV distribution. Various kernel design methods are discussed in [5, 6]

3. COHEN'S CLASS KERNEL DESIGN

Initially many fixed kernels were used for Cohen's class distributions. Kernels designed by Choi and Williams [6] and

978-0-9928626-3-3/15/$31.00 ©2015 IEEE

by Papandreou and Boudreaux-Bartels [7] and recently proposed radial kernels [8] are examples to these kind of kernels. But later it was realized that the signal dependent kernels can produce higher resolution and a kernel design method was proposed by Jones and Baraniuk [9]. The kernel is obtained by solving the following optimization problem,

$$\max_{\Phi^p} \int_0^{2\pi} \int_0^{\infty} |A_x^p(r,\phi)\Phi^p(r,\phi)|^2 r dr d\phi, \tag{4}$$

$$\text{subject to } \frac{1}{4\pi^2} \int_0^{2\pi} \int_0^{\infty} |\Phi^p(r,\phi)|^2 r dr d\phi$$

$$= \frac{1}{4\pi^2} \int_0^{2\pi} \sigma^2(\phi) d\phi \leq \alpha, \quad \alpha \geq 0, \tag{5}$$

where, $A_x^p(r,\phi) = A_x(r\cos\phi, r\sin\phi)$ and $\Phi^p(r,\phi)$ represents the ambiguity function and the kernel in polar coordinates. Since ambiguity function is an auto-correlation function its values around the origin $(r,\phi) = (0,0)$ corresponds to main or the auto-components of a multi-component signal in general [9]. The cross-terms are usually located away from the origin. For this reason in (4) the kernel is taken as a low-pass Gaussian filter and $\sigma^2(\phi)$ represents the variance of the kernel with respect to the angle in polar representation.

With the optimization in (4) the auto-components are selected as much as possible within the low-pass Gaussian filter while with the constraint in (5) the pass-band area of the filter is limited to α to filter out the cross-terms which are located away from the origin. The desired resolution and the cross term attenuation is determined by a proper selection of α.

4. KERNEL ESTIMATION BY PROJECTION ONTO THE EPIGRAPH SET

The kernel design method explained in Section 3 is a multivariable optimization method requiring an iterative solution. In this respect, it is a computationally intensive method compared to the basic WV computation. In this section an alternative method is proposed for the estimation of a signal dependent kernel.

In many signal processing applications an initial rough processing reveals some important features of the analyzed signal, and this will ease the subsequent processing. In Figure 1 two TF distributions that are obtained with fixed and rough initial kernels are shown. The bottom left distribution is obtained with a circular kernel having radius $r = r_0 = N/16$ and the bottom right one is obtained with a Gaussian kernel having the angular standard deviation $\sigma(\phi) = N/16$, where N represents the length of the discrete signal obtained by sampling the signal $x(t)$. The top left distribution is the ideal or desired model TF distribution corresponding to the signal and the top right is the WV distribution. In this figure, there is no adaptation to the signal and both TF distributions are far from the desired or model distribution. But, compared to the

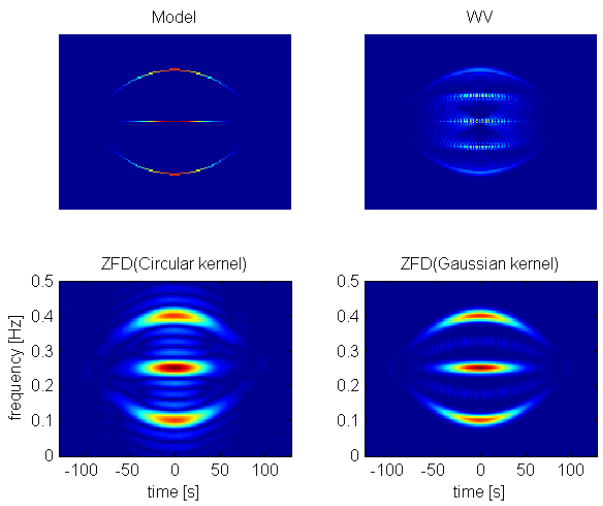

Fig. 1. The desired model corresponding to the signal (top left), WV distribution (top right), TF distribution with circular ($r_0 = N/16$) kernel (bottom left) and the Gaussian ($\sigma(\phi) = N/16$) kernel (bottom right), where N is the length of the discrete-time signal.

WV distribution we observe that the signal has three components and their positioning in TF plane is roughly identified. The fixed kernel TF distributions shown in Figure 1 are, in a sense, noisy and smeared versions of the model TF we are looking for. Therefore, considering localization and spurious structures or cross-terms, they do not carry the the constraints that we desire and need to be regulated. The way of regularization is to project these TF distributions onto a set which contains members having desired constraints. In fact the initial masking with fixed kernels is also a projection. That is, the projection onto the set of TF distributions whose AF values outside the mask are zero. Similar to normal de-noising applications the way of filtering out the high frequency signal terms is to pass the signal through a low pass filter whose passband covers the most of the energy of the actual signal. This operation is a projection onto set of low pass signals containing noiseless signal. In our case we would like to have a signal which has high resolution or localization in TF plane. High localization or resolution in TF plane can be obtained by constraining the l_0 or l_1 norm of the distribution. Therefore we can get a high resolution distribution by projecting the initial fixed kernel TF distribution onto the epigraph or level set of the l_1 norm as shown in Figure 2 where $\boldsymbol{P}$ represents an $N \times N$ matrix corresponding to discrete time and frequency version of the distribution given in (2) and $vec(\boldsymbol{P}) \in R^{N^2}$ represents its vector form. $\boldsymbol{w} \in R^{N^2+1}$ is vector in lifted domain compared to R^{N^2}. If we denote the TF distribution that we have obtained in Figure 1 with fixed kernel as $\boldsymbol{P}_0$, then we can write,

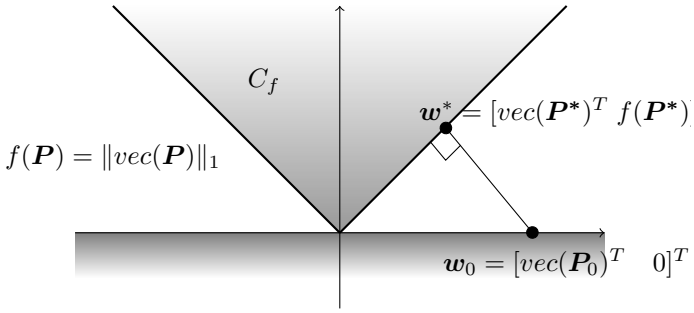

Fig. 2. Geometric description of the projection onto the epigraph set of l_1 norm, where $vec(\boldsymbol{P}) \in \boldsymbol{R}^{N^2}$, and $\boldsymbol{w} = [vec(\boldsymbol{P})^T \quad v]^T \in \boldsymbol{R}^{N^2+1}$ is defined in lifted domain.

$$\boldsymbol{P}_0 = \mathcal{F}\{\boldsymbol{A}_x \bullet \boldsymbol{\Phi}_0\}, \tag{6}$$

where $\boldsymbol{\Phi}_0$ is the matrix corresponding to the fixed kernel and $\boldsymbol{A}_x$ is the matrix corresponding to the ambiguity function of the signal. $\mathcal{F}\{\}$ represents the Fourier transform and '$\bullet$' denotes the element-by-element or Hadamard product.

The epigraph set of the l_1 norm shown in Figure 2 is defined as:

$$C_f = \{\boldsymbol{w} = [vec(\boldsymbol{P})^T \quad v]^T \in \boldsymbol{R}^{N^2+1} \mid f(\boldsymbol{P}) = \|vec(\boldsymbol{P})\|_1 \leq v\} \tag{7}$$

The orthogonal projection of the initial TF distribution $\boldsymbol{P}_0$ onto the epigraph set of l_1 norm is given by,

$$\boldsymbol{P}^* = \min_{\boldsymbol{P} \in C_f} \|vec(\boldsymbol{P}) - vec(\boldsymbol{P}_0)\|_2^2, \tag{8}$$

where the projection, as shown in Figure 2, is obtained with vectors $\boldsymbol{w}_0, \boldsymbol{w}, \boldsymbol{w}* \in R^{N^2+1}$ in lifted domain corresponding to the vectors $\boldsymbol{P}_0, \boldsymbol{P}, \boldsymbol{P}* \in R^{N \times N}$. The implementation of the projection is explained in [10, 11] and [12]. The initial fixed kernel TF distribution $\boldsymbol{P}_0$ and the related projected TF distribution $\boldsymbol{P}^*$ are shown in Figure 3 for two example signals.

As can be seen from Figure 3, the TF representations obtained by projection are over localized and far from the model that we desire. It seems that they corresponds to most localized part of the signal in TF plane. But it is experimentally observed that the projections have an alignment and positioning similar to the signal. In other words they still carry some information related to the signal. Again it is observed that if we get the AF function corresponding to the epigraph projection with inverse Fourier transform as $\boldsymbol{A}^* = \mathcal{F}^{-1}\{\boldsymbol{P}^*\}$ and normalize with its maximum magnitude as $\tilde{\boldsymbol{\Phi}}_x = \frac{|\boldsymbol{A}^*|}{\max_{k,l} |\boldsymbol{A}^*[k,l]|}$ it will give us a signal dependent kernel estimate and this kernel will have an alignment similar to that of the signal in AF domain. In Figure 4 the initial fixed kernel and the estimated kernels for two example signals are shown. In Figures 5 and 6

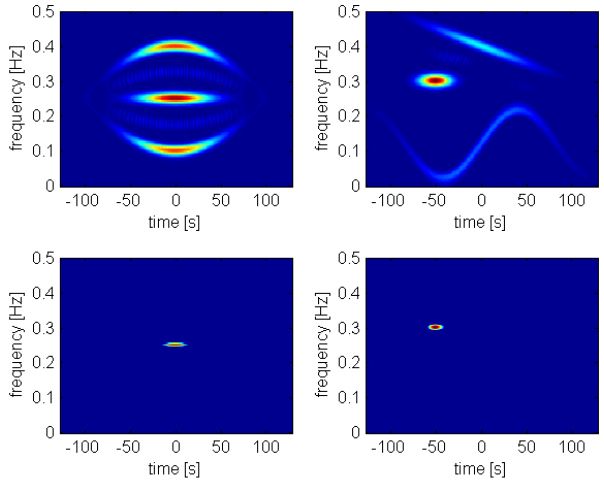

Fig. 3. The initial TF distribution $\boldsymbol{P}_0$ (top) and the TF distribution $\boldsymbol{P}^*$ (bottom) obtained by projection onto epigraph set of l_1 norm for two signal examples.

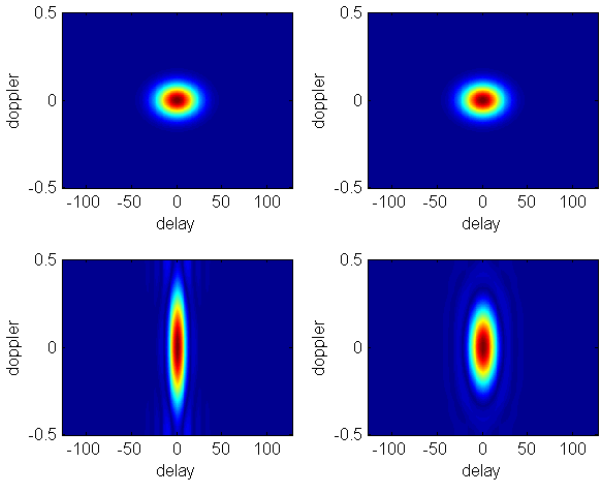

Fig. 4. The initial fixed Gaussian kernel (top) and the signal dependent kernels obtained by projection onto the epigraph set of l_1 norm for two example signals.

the initial TF distributions obtained with fixed kernel and the TF distributions obtained with estimated kernels are shown. For the sake of comparison the model or desired TF distributions and the TF distribution obtained with optimization in (4) are also shown. Figures 5 and 6 shows that compared to the fixed kernel TF distribution, the TF distribution with estimated kernel has higher resolution and does not contain cross-terms. Also, it is observed that the TF distribution with estimated kernel has a comparable result to TF distribution obtained with optimization in (4).

Although a fine tuning is not needed for the selection of

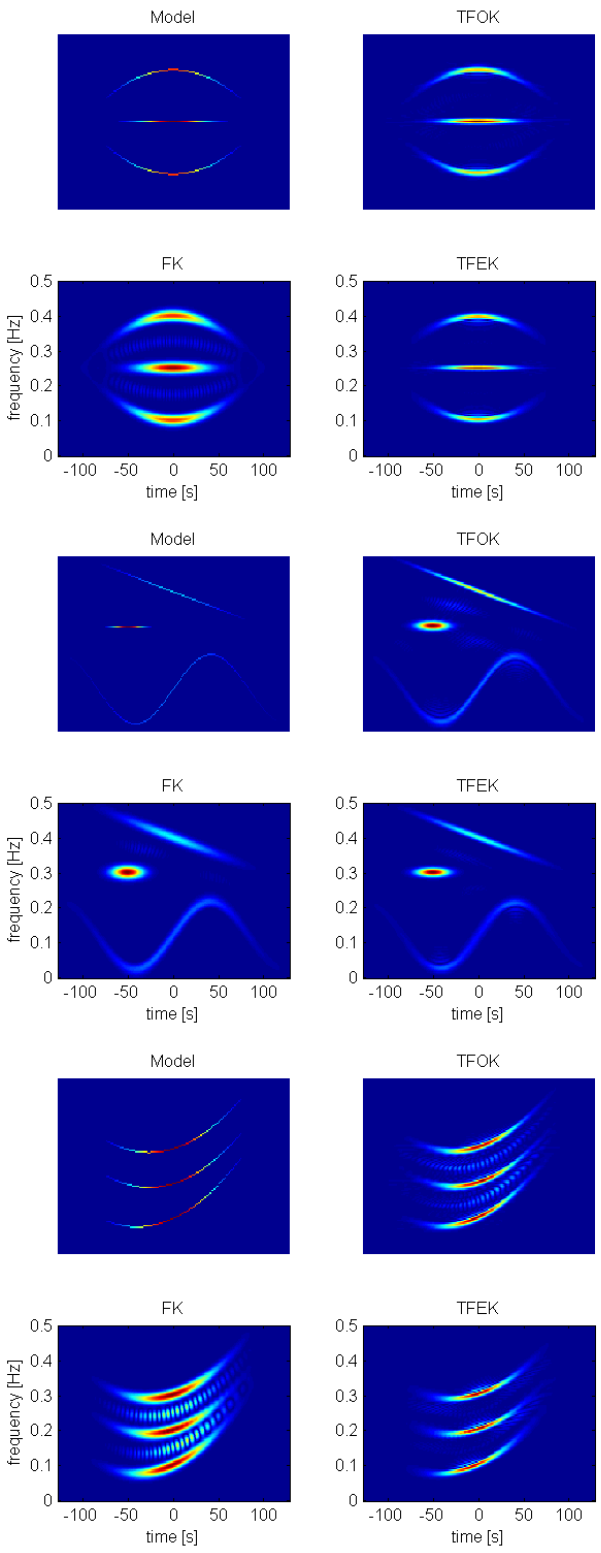

Fig. 5. Comparison of TF distributions obtained by kernel estimation for there example signals. Model: the model TF distribution, TFOK: The TF distribution obtained by kernel optimization in (4) with $\alpha = 1.4$, FK: TF distribution by initial fixed kernel, TFEK: The TF distribution by kernel estimation using projection onto epigraph set of l_1 norm.

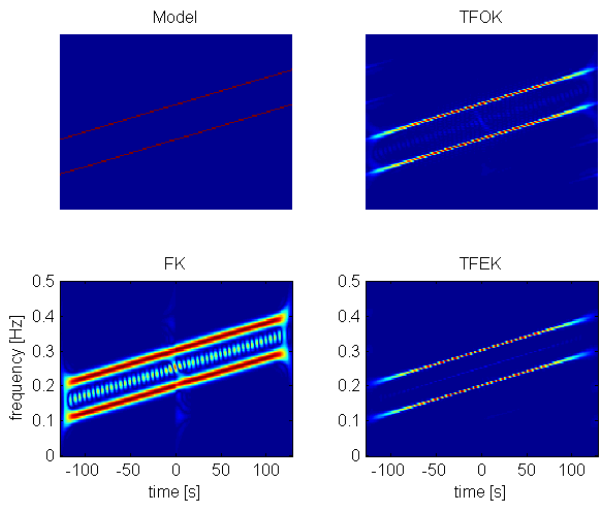

Fig. 6. The comparison of TF distribution for two chirp signals. Model: the model TF distribution, TFOK: The TF distribution obtained by kernel optimization in (4) with $\alpha = 1.4$, FK: TF distribution by initial fixed kernel, TFEK: The TF distribution by kernel estimation using projection onto epigraph set of l_1 norm.

the initial fixed kernel, it will have an effect on the final TF distribution with the estimated kernel. After testing various examples it is experimentally observed that in some cases there are some spurious terms in final TF distribution with estimated kernel. It is also observed that such terms can be eliminated with the selection of initial kernel having an even smaller standard deviation than $\sigma(\phi) = N/16$. But this is another matter of optimization. Also, such a fine tuning is a contradiction to our initial rough and fixed kernel selection idea. Therefore it has not been preferred. It is also observed that such terms can be eliminated with applying a mask or filter $\boldsymbol{G}$ to the initial TF distribution $\boldsymbol{P}_0$ obtained with fixed kernel. This mask is also selected as Gaussian with kernel set to $\sigma(\phi) = N/4$. Therefore this second approach is preferred. Including this mask in TF domain, the steps of overall method for obtaining a high resolution TF distribution based on the projection onto the epigraph set of l_1 norm are given in Table 1.

In Table 2 the similarity and localization or resolution of TF distributions in Figures 5 and 6 are given. The similarity is measured using Pearson Correlation of the vectors corresponding to TF distributions and takes the values in the range [0,1]. The localization or resolution is measured using Renyi entropy [13]. A lower Renyi entropy indicates a better localization or resolution. As can be seen from the Table 2, for all the example signals the similarity and the localization of the proposed kernel estimation based method is comparable to that of the TF distribution obtained with optimization in (4). In order to get good results for all of the tested exam-

Step	Action
1	$\boldsymbol{A}_0 = \boldsymbol{A}_x \bullet \boldsymbol{\Phi}_0$
2	$\boldsymbol{P}_0 = \mathcal{F}\{\boldsymbol{A}_0\}$
3	$\boldsymbol{P}_1 = \boldsymbol{G} \bullet \boldsymbol{P}_0$
4	$\boldsymbol{P}^* = \min_{\boldsymbol{P} \in C_f} \|vec(\boldsymbol{P}) - vect(\boldsymbol{P}_1)\|_2^2$
5	$\boldsymbol{A}^* = \mathcal{F}^{-1}\{\boldsymbol{P}^*\}$
6	$\tilde{\boldsymbol{\Phi}}_x = \frac{\|\boldsymbol{A}^*\|}{\max_{k,l} \|\boldsymbol{A}^*[k,l]\|}$
7	$\tilde{\boldsymbol{P}}_x = \mathcal{F}\{\tilde{\boldsymbol{\Phi}}_x \bullet \boldsymbol{A}_x\}$

Table 1. The steps of overall method for obtaining a high resolution TF distribution using the projection onto the epigraph set of l_1 norm

	Similarity to model/ **Localization**			
Signal	**Model**	**FK**	**TFEK**	**TFOK**
Signal 1	1 / **8.13**	0.44 / **11.32**	0.60 / **10.13**	0.60 / **10.19**
Signal 2	1 / **7.46**	0.41 / **10.87**	0.47 / **10.31**	0.48 / **10.15**
Signal 3	1 / **8.24**	0.39 / **11.45**	0.42 / **10.37**	0.42 / **10.40**
Signal 4	1 / **8.99**	0.39 / **12.38**	0.51 / **9.85**	0.55 / **10.41**

Table 2. The similarity to the model / Renyi entropy values of the TF distributions for the tested example signals

ples, the parameter α in kernel optimization with (4) was set to $\alpha = 1.4$. Further examples can be found in [14].

5. CONCLUSION

A non-iterative kernel design method is proposed for Cohen's class TF distributions. The method is based on the projection onto the epigraph set of l_1 norm. Kernel design results obtained with proposed method are comparable to the results obtained by kernel optimization. Since most signals are sparse in TF domain the proposed l_1-norm based approach reduces cross-terms which clutter the TF plane.

REFERENCES

[1] S. Barbarossa and A. Scaglione, "Adaptive time-varying cancellation of wideband interferences in spread-spectrum communications based on timefrequency distributions," *IEEE Trans. Signal Process.*, vol. 47, no. 4, pp. 879–898, 2005.

[2] D. R. Wehner, *High-Resolution Radar (2nd ed.)*, Artech House, Boston, 1994.

[3] F. Hlawatsch and G.F. Boudreaux-Bartels, "Linear and quadratic time-frequency signal representations," *IEEE Signal Process. Mag.*, vol. 9, no. 2, pp. 21–67, 1992.

[4] T. A. C. M. Claasen and W. F. G. Mecklenbraiuker, "The Wigner distribution - A tool for time-frequency signal analysis; part III: relations with other time-frequency signal transformations," *Philips Journal of Research*, vol. 35, no. 6, pp. 372 – 389, 1980.

[5] L. Cohen, "Time-frequency distributions - a review," *Proc. IEEE*, vol. 77, no. 7, pp. 941–981, 1989.

[6] H. I. Choi and W. J. Williams, "Improved timefrequency representation of multicomponent signals using exponential kernels," *IEEE Trans. Acoust., Speech, Signal Process.*, vol. ASSP37, pp. 862871, June 1989.

[7] A. Papandreou and G. F. Boudreaux-Bartels, "Distributions for time frequency analysis: A generalization of choiwilliams and the butterworth distributions," *IEEE Trans. Signal Process.*, vol. 5, pp. 181184, 1992.

[8] Kodituwakku S., Kennedy R. A., and Abhayapala T. D., "Radial function based kernel design for time-frequency distributions," *IEEE Trans. Signal Process.*, vol. 58, no. 6, pp. 3395–3400, 2010.

[9] Douglas L. Jones and Richard G. Baraniuk, "An adaptive optimal-kernel time-frequency representation," *IEEE Trans. Signal Process.*, vol. 43, no. 10, pp. 2361 – 2371, 1995.

[10] A. E. Çetin, A. Bozkurt, O. Gunay, Y. H. Habiboğlu, K. Kose, R. A. Sevimli, and M. Tofighi, " Projections onto Convex Sets (POCS) Based Optimization by Lifting ," in *1st IEEE Global Conf. Signal Inf. Process.*, Austin, Texas, U.S.A., December 3-5 2013.

[11] Z. Deprem and A. E. Çetin, "Crossterm-free Time-Frequency Distribution Reconstruction via Lifted Projections," *IEEE Trans. Aerosp. Electron. Syst.*, vol. 51, no. 1, pp. 1–13, 2015.

[12] G. Chierchia, N. Pustelnik, J.-C. Pesquet, and B. Pesquet-Popescu, "An epigraphical convex optimization approach for multicomponent image restoration using non-local structure tensor," in *IEEE Int. Conf. Acoust., Speech Signal Process. (ICASSP)*, 2013, pp. 1359–1363.

[13] R. G. Baraniuk, P. Flandrin, A. J. E. M. Janssen, and O. Michel, "Measuring time-frequency information content using the Rényi entropies," *IEEE Trans. Inf. Theory*, vol. 47, no. 4, pp. 1391–1409, 2001.

[14] Z. Deprem, *Sparsity and Convex Programming in Time-frequency Processing*, Ph.D. thesis, Bilkent University, Ankara,Turkey, 2014.